Constitutive models to describe the mechanical behavior of salt rocks and the imbedded weakness planes

W. Minkley & J. Mühlbauer
Institut für Gebirgsmechanik GmbH, Leipzig, Germany

ABSTRACT: Up to now salt rock mass has been predominantly regarded as a continuum and the mechanical effect of the present discontinuities and bedding planes have been neglected to a great extent. However, for a complete understanding of a couple of geomechanical phenomena this approach proves to be insufficient. When solving numerous practical problems in potash and rock salt mining it clearly turned out that a treatment without taking the existing bedding planes and discontinuities into account will not provide a satisfying explanation of the observed rock mechanical processes. Therefore, for a mechanical description of the complex properties of the salt rock mass a visco-elasto-plastic constitutive model is presented, which comprises the hardening/softening behavior and dilatancy effects for salt rocks, as well as a specific friction model, which comprises displacement- and velocity-dependent shear strength softening for salt bearing bedding planes.

1 INTRODUCTION

Generally, when rock mechanical problems are studied, the salt rock mass is regarded as a continuum and a special emphasis is given to its visco-plastic behavior. However, it does not prove possible to describe comprehensively the stability behavior of mine cavities in salt rocks solely on the basis of the viscous properties and, for instance, time-dependent softening effects.

When investigating the in situ observed fracture and dilatancy processes in chamber horizons, it turned out that the observed significant floor heave movements are linked with mechanically activated weakness surfaces and bedding planes in the mining floor. Such intensive floor lift phenomena have been observed in numerous cases, e.g. before the heavy rock burst in a trona (a water-bearing sodium carbonate compound) salt mine in Wyoming, which happened in 1995 (Swanson & Boler 1995), and before the rock burst with a similar magnitude in 1996, which destroyed the eastern mining field of the Teutschenthal salt mine in the central area of Germany.

The mechanisms of floor lifts and the development of relevant failure processes in the working floor are closely connected with the softening and dilatancy properties of the solid salt rocks and with the existing bedding planes which can act as sliding faces. They are just those weakness planes at a short distance to the mined cavity which actually allow a significant softening process (Fig. 1). If fracture processes happen inside the working floor, shear displacements occur on the bedding planes within this zone. The extent of the heave movement essentially depends on the distance between the bottom of the cavity and the present bedding planes or discontinuity surfaces, respectively. It further depends on the chamber width, on the age of the working panel, and on the mechanical properties of the solid salt rock and the imbedded weakness planes.

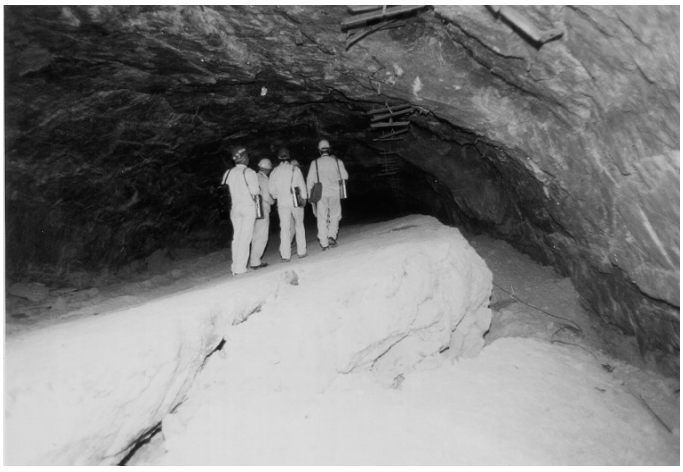

Figure 1. Extreme floor lifts caused by numerous bedding planes in the floor.

On existing discontinuities between viscous salt rock and such layers which are not able to creep like high-strength anhydrite rock beds, high shear stresses can occur as well as rupture processes of consi-

derable magnitude. This way, when in 1975 above the former Neustassfurt potash mine a large sinkhole developed as a result of a progressive caving to the surface, slide processes have played a decisive role (Salzer et al. 2004). These slide processes occurred between the Stassfurt potash seam in steep stratification and the so-called main anhydrite which is found in the roof. By means of micro-seismic monitoring such shear movements and separation processes, respectively, between rock salt and the subjacent main anhydrite can be detected by measurements of acoustic emission (Spies et al. 2004).

In potash mining the contact properties of the bedding planes to the hanging and underlying salt bedrock affect the load bearing behavior of pillars to a considerable extent. The triaxial constraint of the pillars and, thus, their maximum bearing capacity are transmitted via the mechanical contact conditions at the transition to the surrounding rock masses. Depending on the properties of the solid salt rocks and the existent bedding planes, shear displacements on the contact zones can occur either slowly or abruptly, in connection with contour failure processes or even a pillar collapse.

For assessing the safety and the stability of mine openings in salt rocks the mechanical behavior of bedding planes is of high practical importance. However, on this behavior very little research work has been done up to now. In cases where the roof or floor is stratified, the contour stability of cavities is essentially determined by the mechanical properties of the bedding planes. This way, the observed collapse of compact pillars in potash mining can only be understood, when a loss in cohesion and of adhesive friction on the contact to the surrounding salt rock mass is taken into consideration.

Figure 2. Softening phenomena within the rock and on horizontal bedding planes of a hard salt pillar.

Particularly, under dynamic loading conditions just those mechanical properties of the salt rock mass get decisive significance which represent its discontinuum-mechanical attributes. These properties have been induced already during the saline sedimentation or later by tectonic processes. Therefore, for a comprehensive treatment of corresponding rock mechanical problems it is required to describe the softening behavior of both, the salt rocks and the imbedded weakness planes (Fig. 2).

Therefore, in the following, first of all a visco-elasto-plastic constitutive model for salt rocks is presented which has been developed in the Institute for Rock Mechanics, Leipzig. This constitutive model implies both hardening/softening behavior and dilatancy. Subsequently, a shear model including displacement- and velocity-dependent softening for the application in salt formation with bedding planes is presented.

2 VISCO-ELASTO-PLASTIC CONSTITUTIVE MODEL FOR SALT ROCKS

A constitutive model for salt rocks must comprise the following deformation properties (Döring et al. 1964):

- reversible time-independent deformation components (elasticity);
- reversible time-dependent deformation components (persistence);
- irreversible permanent deformation components (viscosity, plasticity).

Whereas plasticity is predominantly an attribute of polycrystalline rocks, viscosity is more a characteristical feature of non-crystalline structures.

Moreover, salt rocks – like other rock materials too – exhibit softening phenomena. Softening in this context stands for the decrease of strength of the rock material, when deformation is increasing (strain softening). Under this aspect, in dependence on the rock properties and the loading conditions, different features in their behavior appear. When an abrupt softening occurs, the phenomenon is called brittle fracture, whereas if gradual softening occurs the material presents yield failure behavior. So, perfect plastic yield is interpreted as deformation without any softening.

In the physical sense, softening is caused by the generation and accumulation of microcracks and defects within the rock material which progressively develop to macrocracks. During this process, the strength drops to a certain residual level. This residual strength is mainly due to friction processes which run on the formed macroscopic fracture surfaces. Thus, this residual strength is regarded as the lower yield limit of the rock material in the post-failure state.

In the developed constitutive model the plastic behavior implying the softening of the polycrystalline salt rocks is described by a modified non-linear Mohr-Coulomb yield or failure criterion using a non-

associated flow rule. The Mohr-Coulomb fracture hypothesis in which the yield point and failure limit depend on the minimal principal stress σ_3 is generally accepted for rock materials.

A failure criterion which satisfies the above mentioned demands on the basis of a modification of the Mohr-Coulomb model has been developed by Minkley (1997):

$$\sigma_{1,B} = \sigma_D + N_\phi \cdot \sigma_3 \tag{1}$$

with the function for friction:

$$N_\phi = 1 + \frac{\sigma_{MAX} - \sigma_D}{\sigma_\phi + \sigma_3} \tag{2}$$

respectively,

$$\sigma_{eff,B} = \sigma_D + \frac{\sigma_{MAX} - \sigma_D}{\sigma_\phi + \sigma_3} \cdot \sigma_3 \tag{3}$$

where σ_3 = minimum principal stress; $\sigma_{1,B}$ = maximum principal stress at failure; $\sigma_{eff,B} = \sigma_{1,B} - \sigma_3$ = maximum effective stress at failure; $\sigma_D(\varepsilon^p)$ = uniaxial strength; $\sigma_{MAX}(\varepsilon^p)$ = maximum effective strength; $\sigma_\phi(\varepsilon^p)$ = curvature parameter for strength surface; and ε^p = plastic shear deformation.

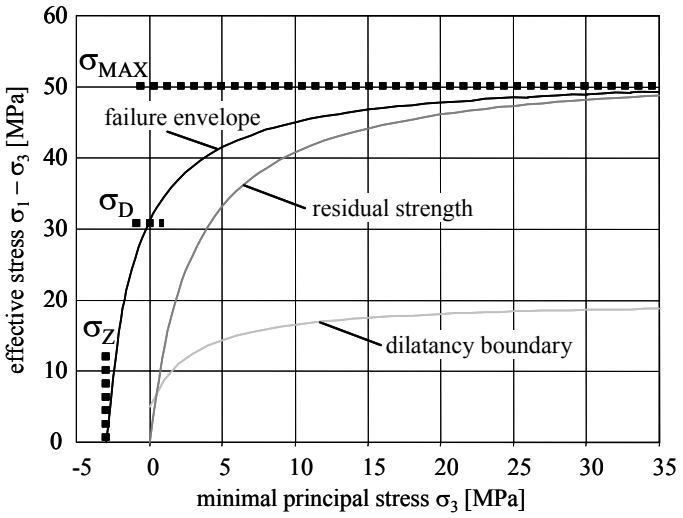

Figure 3. Yield points in the visco-elasto-plastic constitutive model.

For clarification of the function of the respective parameters compare Figure 3 where the failure criterion is plotted as $\sigma_1 - \sigma_3 = f(\sigma_3)$. σ_{MAX} is the maximum effective stress the rock can carry and to which the failure criterion moves towards with increasing minimum principal stress σ_3. For salt rocks under mining conditions the non-linearity of the failure envelope can not be ignored. The non-linear failure criterion describes both compression and tension. More precisely, the tensile strength is given by:

$$\sigma_Z = \sqrt{\frac{1}{4}\left(\sigma_\phi + \sigma_{MAX}\right)^2 - \sigma_D \cdot \sigma_\phi} - \frac{1}{2} \cdot \left(\sigma_\phi + \sigma_{MAX}\right) \tag{4}$$

From the modified non-linear Mohr-Coulomb failure criterion (Eq. 3), the flow rule for plastic flow can be deduced (pressure with negative sign):

$$f_S = \sigma_1 - \sigma_3 + \sigma_D - \frac{\sigma_{MAX} - \sigma_D}{\sigma_\phi - \sigma_3} \cdot \sigma_3 \tag{5}$$

The plastic potential for non-associated flow is given by:

$$g_S = \sigma_1 - \sigma_3 - \frac{\sigma_{MAX,\psi} - \sigma_D}{\sigma_\psi - \sigma_3} \cdot \sigma_3 \tag{6}$$

where $\sigma_{MAX,\psi}(\varepsilon^p)$ = maximum effective strength at the dilatancy boundary; and $\sigma_\psi(\varepsilon^p)$ = curvature parameter of the dilatancy function.

If the failure envelope is reached, plastic deformations occur in addition to the elastic deformations. Using the flow rule, the plastic incremental deformation part can be determined:

$$\Delta\varepsilon_i^p = \lambda_S^* \cdot \frac{\partial g_S}{\partial \sigma_i} \qquad i = 1,3 \tag{7}$$

Besides the elasto-plastic characteristic, most salt rocks show viscous behavior. Therefore, the elasto-plastic softening model is already combined with the Burgers creep model. The incremental form of the Burgers model is given in the *FLAC* manuals (Itasca 1998). The determination of the multiplier λ^*_S in Equation (7) is obtained for $f_S = 0$:

$$\lambda_S^* = \frac{\sqrt{C_4^*} - C_2^*}{2 \cdot C_1^*} \tag{8}$$

$$C_1^* = -\frac{1}{\sigma_\phi}\left(\alpha_2 - \alpha_1 \cdot N_\psi\right) \cdot \left[\left(\alpha_2 - \alpha_1 \cdot N_\psi\right) - \left(\alpha_1 - \alpha_2 \cdot N_\psi\right)\right]$$

$$C_2^* = -\frac{1}{\sigma_\phi}\left(\alpha_2 - \alpha_1 \cdot N_\psi\right) \cdot \left(\sigma_1 - 2 \cdot \sigma_3 + \sigma_{MAX} + \sigma_\phi\right)$$

$$+ \left(\alpha_1 - \alpha_2 \cdot N_\psi\right) \cdot \left(1 - \frac{\sigma_3}{\sigma_\phi}\right)$$

$$C_3^* = \frac{\sigma_3}{\sigma_\phi} \cdot \left(\sigma_1 - \sigma_3 + \sigma_{MAX}\right) - \left(\sigma_1 - \sigma_3 + \sigma_D\right)$$

$$C_4^* = C_2^{*2} - 4 \cdot C_1^* \cdot C_3^*$$

$$\alpha_1 = K + \frac{2}{3 \cdot a} \qquad \alpha_2 = K - \frac{1}{3 \cdot a}$$

$$a = \frac{1}{2 \cdot G^M} + \frac{\Delta t}{4} \cdot \left(\frac{1}{\eta^M} + \frac{1}{A^* \cdot \eta^K}\right)$$

$$A^* = 1 + \frac{G^K \cdot \Delta t}{2 \cdot \eta^K}$$

N_ψ is the dilatancy function:

$$N_\psi = 1 + \frac{\sigma_\psi^2}{(\sigma_\psi - \sigma_3)^2} \cdot \tan\beta_0 \qquad (9)$$

where $\tan\beta_0$ and σ_ψ depend on the plastic deformation ε^p.
For volume increase (dilation) is valid:

$$\frac{\Delta V}{V_0} = \varepsilon^p_{Vol} = (N_\psi - 1) \cdot \varepsilon^p \qquad (10)$$

The parameters which describe the dilatancy are: $\beta_0(\varepsilon^p)$ = ascent angle of the dilatancy curve; $\varepsilon^p{}_{Vol}$ = $f(\varepsilon^p)$ at uniaxial loading ($\sigma_3 = 0$); and $\sigma_\psi(\varepsilon^p)$ = curvature parameter of the dilatancy function.

The model allows to describe the creep behavior including creep rupture. The primary creep phase is modelled by the Kelvin model with Kelvin shear modulus G^K and Kelvin viscosity η^K. The secondary creep phase is controlled by the Maxwell viscosity η^M. The tertiary creep phase is governed by a dilation softening mechanism. Under the assumption that $\eta^K \to \infty$ and $\eta^M \to \infty$ (i.e. no viscous deformation) the equations in (8) yield

$$a = \frac{1}{2 \cdot G^M}$$

and the material behavior coincides with the time-independent elasto-plastic model section. Within the visco-elasto-plastic material model, the stress dependency of the creep rate is governed by the exponential dependency of the Maxwell viscosity η^M on the deviatoric stress σ_V (Lux 1984):

$$\eta^M = \eta_0^M \cdot e^{-m \cdot \sigma_V} \qquad (11)$$

In the constitutive model the short-time and the long-time strengths are taken into consideration by a yield limit which depends on the deformation rate.

The rock mechanical quantities which determine this limit are the compressive strength σ_D at $\sigma_3 = 0$ and the maximum effective strength σ_{MAX} at $\sigma_3 \to \infty$ (Fig. 3). Both quantities depend on the deformation rate $\dot{\varepsilon}$. On the basis of results obtained in experimental tests on different salt rocks the following relationships have been introduced for this purpose:

$$\sigma_D(\dot{\varepsilon}) = \sigma_D\left(1 + a_M \cdot (f(\dot{\varepsilon}) - 1)\right)$$

$$\sigma_{MAX}(\dot{\varepsilon}) = \sigma_{MAX}\left(1 + a_M \cdot (f(\dot{\varepsilon}) - 1)\right) \qquad (12)$$

with

$$f(\dot{\varepsilon}) = \frac{1}{2}\left(1 + \tanh\left(b_M \cdot \log\frac{\dot{\varepsilon}}{\dot{\varepsilon}_W}\right)\right)$$

The parameters used here have following meaning: a_M = reduction factor short-time strength → long-time strength; b_M = velocity factor; and $\dot{\varepsilon}_W$ = deformation velocity at the inflection point.

In the modified non-linear Mohr-Coulomb plasticity model both the dilatancy boundary and the failure limit are described by the yield function (Equation 3). Here, the dilatancy boundary or damage limit, resp., is regarded as the lower yield envelope in the pre-failure state, whereas the residual strength is regarded as the lower yield limit in the post-failure region. The dependence of the yield limit on both the minimum principal stress σ_3 and on the deformation velocity $\dot{\varepsilon}$ is described in a functional manner while the dependence on the plastic deformation ε^p is given in tables. This procedure allows a universal adaptation to the pronounced non-linear deformation behavior of the salt rocks.

In Figure 4 the concept of the model is illustrated. This model distinguishes between 4 different deformation components, the sum provides the total magnitude of deformation ε.

Below the dilatancy boundary the deformation is composed of the following components:

$$\varepsilon = \varepsilon^e + \varepsilon^{en} + \varepsilon^v \qquad (13)$$

Above the dilatancy limit the total deformation is given by:

$$\varepsilon = \varepsilon^e + \varepsilon^{en} + \varepsilon^v + \varepsilon^p \qquad (14)$$

Both the elastic deformation component ε^e and the component of the elastic persistence ε^{en} are reversible quantities whereas both the viscous (ε^v) and the plastic portions of deformation ε^p are irreversible quantities.

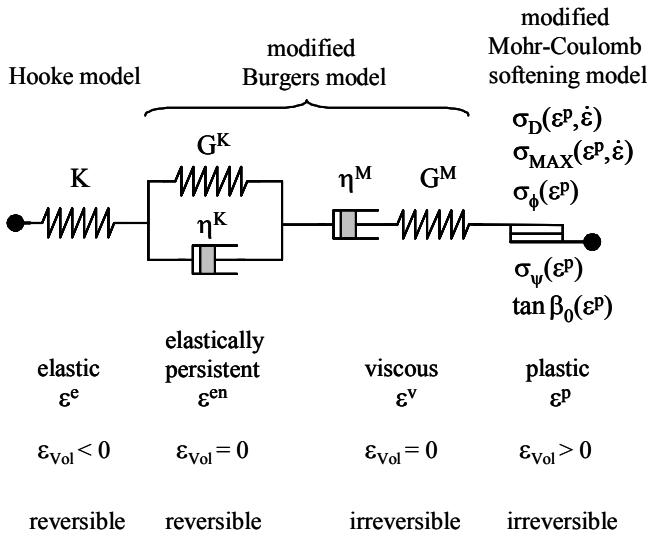

Figure 4. Visco-elasto-plastic model concept.

Furthermore, in the model it is assumed that volume expansion is only provided by the elastic and the plastic volumetric deformation components:

$$\varepsilon_{Vol} = \varepsilon^{e}_{Vol} + \varepsilon^{p}_{Vol} \tag{15}$$

Then, in the case of compression, volume compaction occurs below the dilatancy limit ($\varepsilon^{e}_{Vol} < 0$), whereas plastic volume dilatation due to damaging processes will occur, when the dilatancy limit is exceeded, $\varepsilon^{p}_{Vol} > 0$. At the dilatancy boundary applies:

$$\frac{d\varepsilon_{Vol}}{d\varepsilon} = 0$$

Salt rocks possess elastic as well as plastic and viscous properties which are superimposing each other. The presented concept (Fig. 4) of the visco-elasto-plastic constitutive model is based on the well accepted standard models of mechanics. This concept is applicable in a universal manner to both, salt rocks and non-saline rock materials too. The explained constitutive model is suitable for the description of the time-dependent mechanical behavior of salt rocks presenting both ductile and brittle material behavior.

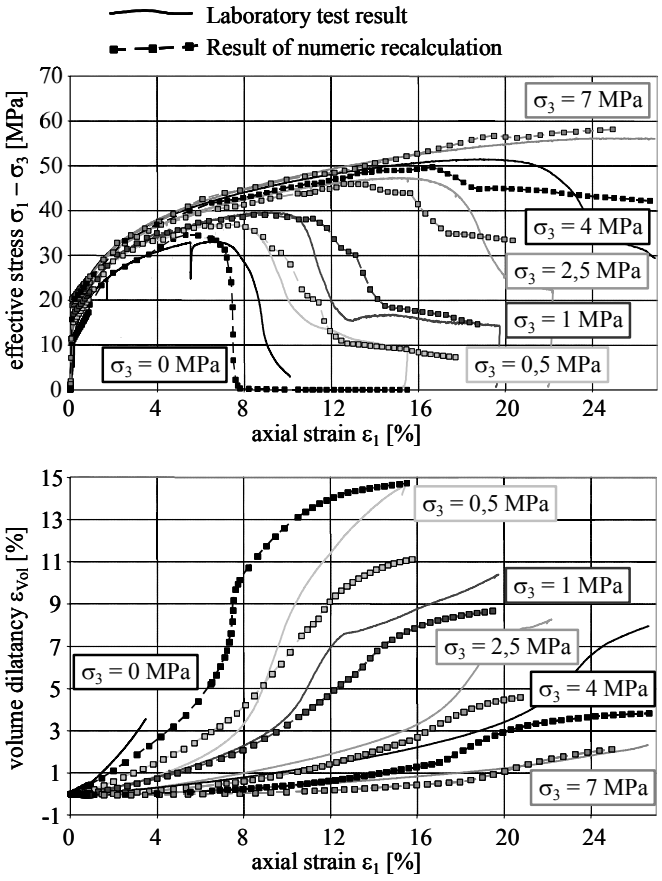

Figure 5. Recalculation of strength tests carried out on rock salt. Upper part: stress-strain curves; lower part: dilatancy curves.

In Figure 5 a comparison is shown between the stress-strain curves, which are obtained in laboratory tests on several rock salt specimens under uniaxial and triaxial loading conditions, and the results of the corresponding numerical recalculations. It is quite evident, that the strain-hardening behavior rises with increased confining pressure until the peak strength is reached, and the level of the post-failure stress drop reduces. At higher confining pressures, the dilatancy (Fig. 5, lower part) is heavily depressed. Laboratory test results and numeric recalculations are obviously in a good agreement.

As noted already, the constitutive model also describes the viscous behavior of salt rocks until creep failure. The recalculation of a creep test carried out on a rock salt specimen is shown in Figure 6.

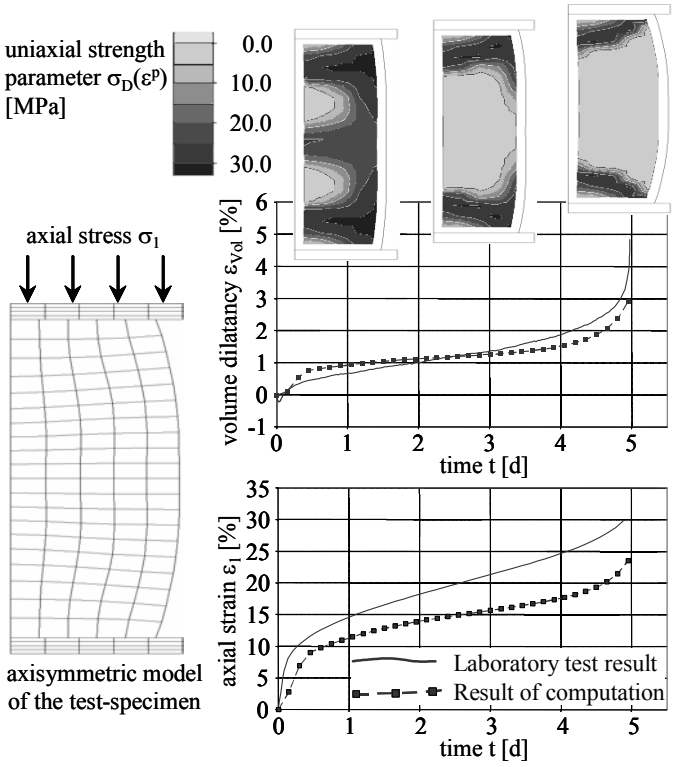

Figure 6. Recalculation of a creep test on a rock salt specimen: axial stress σ_1 = 41 MPa and confining pressure σ_3 = 3 MPa. Time-dependent development of the uniaxial strength parameter σ_D (compare equation 3) within the specimen.

3 SHEAR MODEL FOR BEDDING PLANES

For the understanding of the instability, which is observed in fault zones, on crack surfaces, and bedding planes in the rock mass, it is necessary to describe the softening processes occurring on present mechanical weakness planes. For this purpose, two model concepts are commonly used in geomechanics (Brady 1990):

- velocity-dependent softening (velocity weakening)
- displacement-dependent softening (displacement weakening)

The dependence of friction on the shear rate is known for a long time. As a result, instable sliding on natural rock joints has been accepted. It has to be

noted that the conception, that the dynamic friction coefficient is smaller than the static coefficient, was the starting point for the interpretation of seismic instability (Brace & Byerlee 1966).

Dietrich (1978) has introduced a velocity-depending formulation by means of friction phenomena with respect to the change in the shear resistance or an equivalent friction coefficient: Thus, he can explain the dynamic instability, which is observed in the case of earthquakes, for instance. This formulation has been refined, among others, by Rice (1983) and Ruina (1983). From their analytical solutions it follows that the friction coefficient increases instantaneously, when the sliding rate rises abruptly. But afterwards, the effective friction coefficient drops to a lower level. That means that a velocity-dependent shear softening process becomes active which provokes an unstable sliding.

Displacement-dependent softening models describe the drop of shear strength by assuming the progressive damaging of the unevenness of the joint planes at increasing shear displacement (Cundall & Hart 1984, Indraratna & Haque 2000).

In contrast to most joints in other types of rock, the properties connected with cohesion and adhesive bonds on discontinuities and bedding planes in salt rocks are of special importance – besides the friction itself (Fig. 8). In contrast to rocks like silicatic rock, already under quite normal loading conditions, as they are generally found in a mine, the salt rocks exhibit to a great extent the capability to reactivate adhesive and cohesive forces on reclosed parting planes (Minkley 1989).

A further particularity of the shear behavior on bedding planes in salt rocks, is the evident dependence on the velocity. The developed shear model (IfG 2005), which implies the displacement-dependent and the velocity-dependent strength softening, is based on the concept of Cundell & Lemos (1990). The essential features of the shear model for bedding planes in salt rocks are:

- Dependence of the adhesive friction coefficient on the displacement rate of the shear process
- The shear stress versus shear displacement curve approaches a "target" shear strength of the bedding plane
- The "target" shear strength remains constant until the softening region is reached, then it decreases with the progressing shear displacement.

In the incremental formulation, the shear model can be described as follows. For the relationship between normal loading and normal displacement we use:

$$\Delta\sigma_N = k_N \cdot \Delta u_n \tag{16}$$

where k_N is the normal stiffness and Δu_n is the normal displacement between the joint surfaces.

The model responds to the shear loading with an irreversible non-linear behavior. The shear stress increment is calculated as follows:

$$\Delta\tau = F \cdot k_S \cdot \Delta u_s \tag{17}$$

Here, k_S is the shear stiffness and Δu_s is the shear displacement parallel to the shear plane (Fig. 7).

The factor F which reduces the slope is a function of the distance between the current shear stress τ and the peak shear strength τ_{MAX}:

$$F = 1 - \frac{\tau}{\tau_{MAX}} \tag{18}$$

When taking into account the adhesive friction which is of essential importance for the bedding planes in salt rocks, the shear strength is found to be:

$$\tau_{MAX} = \mu \cdot \sigma_N + c \tag{19}$$

with the friction coefficient:

$$\mu = \mu_K (1 + \Delta\mu)$$

which is consists of the coefficient of the kinetic friction:

$$\mu_K = \tan\left(\phi_R + i_0 \cdot e^{-K2 \frac{\sigma_N}{\sigma_K}} \right) \tag{20}$$

and the coefficient of the adhesive friction:

$$\Delta\mu = \Delta\mu_{vel} \cdot e^{-K1 \frac{\sigma_N}{\sigma_K}} \tag{21}$$

Here are: c = cohesion; ϕ_R = angle of residual friction; i_0 = upslide angle; σ_K = compressive strength in the contact area; and K1, K2 = curvature parameters.

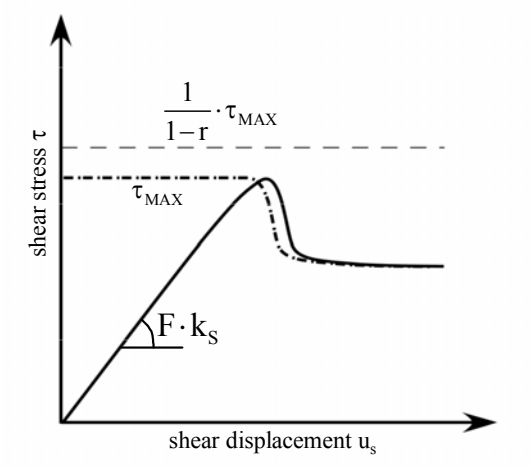

Figure 7. Shear model with strength softening.

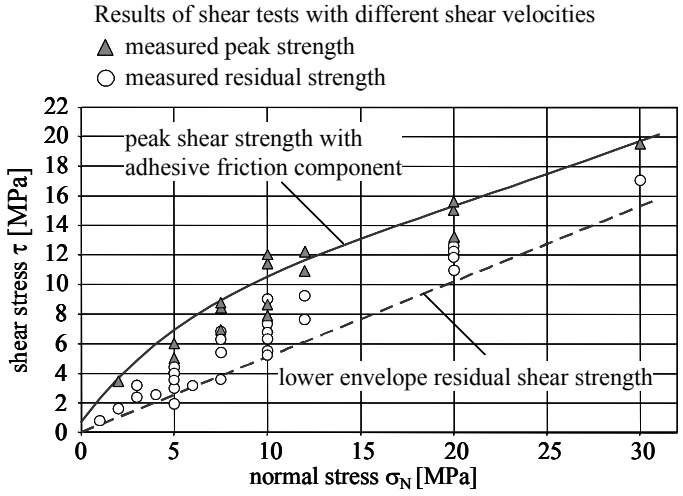

Figure 8. Laboratory test results to determine peak and residual shear strengths on the bedding plane carnallitite / rock salt.

The effects of the kinetic and the adhesive friction components are proportional to the normal loading σ_N on the bedding plane. The cohesion diminishes only during very quick slide processes, whereas during a quite slow shear process the cohesive forces are maintained due to the specific characteristics of the salt which are covered by the rules of the physics of interfaces.

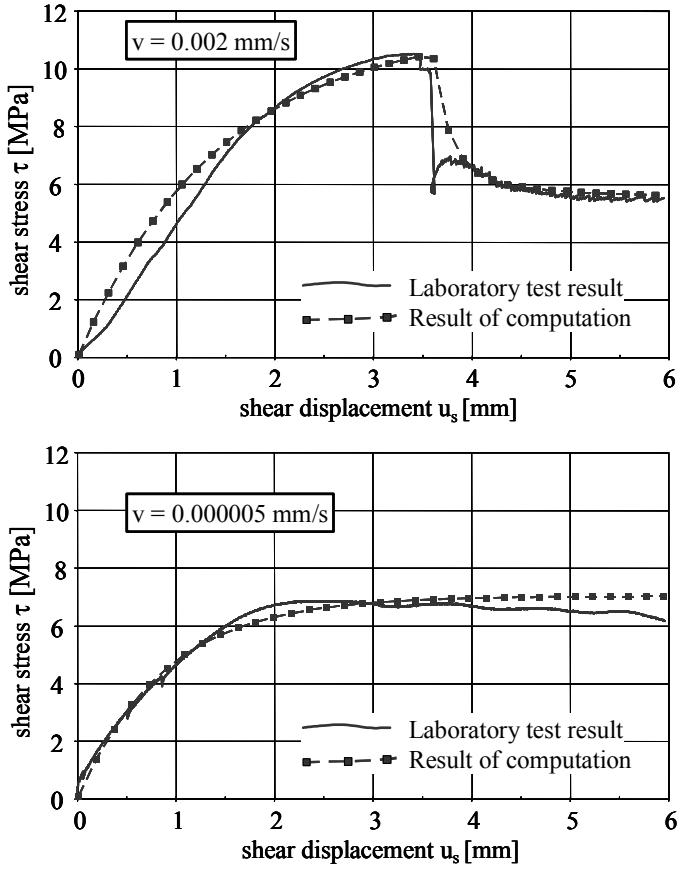

Figure 9. Recalculation of direct shear tests with different shear velocities v on the bedding plane carnallitite / rock salt; Normal loading σ_N = 10 MPa.

The dependence of the friction on the velocity v of the active shear process is represented by the following function:

$$f_{vel}(v) = \frac{1}{2}\left(1 + \tanh\left(b_S \cdot \log\frac{v}{v_K}\right)\right) \tag{22}$$

Accordingly, the velocity-dependent extent inside the adhesive friction coefficient can be expressed by:

$$\Delta\mu_{vel} = \frac{\mu - \mu_K}{\mu_K} = \Delta\mu_{MAX} \cdot f_{vel} \tag{23}$$

In the physical interpretation, this means that in the case of a dynamical slide process at high shear velocities ($f_{vel} \approx 1$) an adhesive friction resistance must be overcome before a loss of strength appears. Under such conditions a significant drop in shear stress occurs (Fig. 9, upper diagram).

In contrast to that, in slow shear processes ($f_{vel} \approx 0$) no additional resistance of adhesive friction develops as in the case of a quick movement and, thus, cohesion is maintained. Such slide processes on the bedding planes run practically without any drop in shear stress (Fig. 9, lower diagram).

Besides the velocity-dependent shear behavior also a strength softening that depends on the passed shear displacement has been taken into consideration, in the developed shear model. As soon as the peak shear strength is approached, a reduction of the adhesive friction component occurs which depends on the plastic shear displacement. When the maximum shear strength τ_{MAX} has been approached up to a certain level r which must be preset, shear softening occurs if the following relationship is valid:

$$\tau \geq (1 - r) \cdot \tau_{MAX} \qquad \text{or} \quad F \leq r \tag{24}$$

The reduction of the adhesive friction along the shear displacement in incremental formulation follows the relationship:

$$\Delta\mu_S^p = -\Delta\mu_{vel} \cdot \frac{\Delta u_s^p}{L1} \tag{25}$$

where the increment of plastic shear displacement is defined by:

$$\Delta u_s^p = (1 - F)\Delta u_s \tag{26}$$

The shear parameter L1 determines the steepness of the shear stress drop in the post-failure region. With increasing shear displacement the peak shear strength will be passed, furthermore, the upslide angle i_0 is lowered to reproduce the abrasion process resulting in a reduction of the unevenness between the joint faces and, additionally, mylonitisation. The difference between the present shear strain and the shear strain to reach the residual shear strength plateau of smoothed shear planes by abrasion is descri-

bed by the parameter L2. For the reduction of the upslide angle in incremental form applies:

$$\Delta i = -i_0 \cdot \frac{\Delta u_s^P}{L2} \tag{27}$$

The incremental Equations (25) and (27) correspond to an exponential reduction of the adhesive friction component and the upslide angle during proceeding shear displacements on the bedding plane in the post-failure state.

The effective dilatancy angle i is calculated as follows:

$$i = \arctan\frac{\tau}{\sigma_N} - \arctan\mu_K \tag{28}$$

Table 1: Shear model parameters for bedding planes carnallitite / rock salt.

Parameter	Symbol	Value	Unit
Residual friction angle	ϕ_R	29	deg
Upslide angle	i_0	5	deg
Compressive strength contact area	σ_K	10	MPa
Curvature parameter 1	K1	1.0	
Curvature parameter 2	K2	0.4	
Cohesion	c	0.7	MPa
Maximum adhesive friction coefficient	$\Delta\mu_{MAX}$	1.5	
Softening distance 1	L1	0.003	m
Softening distance 2	L2	0.08	m
Distance parameter	r	0.08	
Velocity factor	b_S	1.2	
Critical shear velocity	v_K	0.00001	mm/s
Shear stiffness	k_S	8	GPa/m
Normal stiffness	k_N	10	GPa/m

The parameters as required for the shear model are summarised in Table 1. The given quantities have been determined in several direct shear tests which were carried out on bedding planes between carnallitite and rock salt (Fig. 8). For the presented recalculation of some shear tests the *3DEC*-model as shown in Figure 10 has been used.

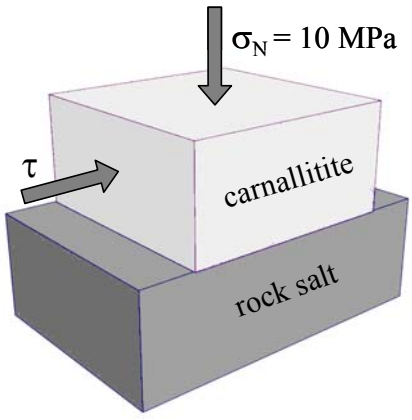

Figure 10. *3DEC*-simulation of shear tests carried out on the bedding plane between carnallitite and rock salt.

4 IMPLEMENTATION AND APPLICATION IN PRACTICE

The visco-elasto-plastic constitutive model implying hardening/softening behavior has been programmed in C++ and is available as a DLL-file (Dynamic Linked Libraries) for high-performance calculation programs in the domains of continuum mechanics and discontinuum mechanics on the basis of:

- finite differences: *FLAC*^{2D}, *FLAC*^{3D}
- distinct elements: *UDEC*, *3DEC*

These programs use an explicit time-step algorithm (Cundall & Board 1988) which is specifically suited for the modelling of non-linear processes and instability problems.

The developed shear model for bedding planes can be implemented as a user-defined joint constitutive model into the computation codes *UDEC* and *3DEC* in the domain of discontinuum mechanics.

Examples of the verification and practical application of the introduced constitutive models will be presented in another paper in this volume (Minkley et al. 2007). The usage of these constitutive models allows to describe the mechanical behaviour of the salt rock mass from the aspects of continuum mechanics as well as discontinuum mechanics.

ACKNOWLEDGEMENTS

The studies presented in this paper were funded by the German Federal Ministry of Research and Education under contracts 02C0264, 02C0639/3 and 02C0892.

We also appreciate the thorough review made by Otto Schulze (BGR) which helped to prepare the final version of the paper.

REFERENCES

Brace, W.F. & Byerlee, J.D. 1966. Stick-slip as a mechanism for earthquakes. *Science* 153: 990-992.

Brady, B.H.G. 1990. Keynote lecture: Rock stress, structure and mine design. In C. Fairhurst (ed.), *Proc. 2nd Int. Symp. on Rockbursts and Seismicity in Mines, Minneapolis, 8-10 June 1990*: 311-321. Rotterdam: Balkema.

Cundall, P.A. & Hart, R.D. 1984. *Analysis of block test no. 1 inelastic rock mass behavior: phase 2 – a characterization of joint behavior (final report)*. Itasca Consulting Group Report, Rockwell Hanford Operations, Subcontract SA-957.

Cundall, P.A. & Board, M. 1988. A Microcomputer Program for Modelling Large-Strain-Plasticity Problems. In G. Swoboda (ed.), *Proc. 6th Int. Conference on* Numerical Methods in Geomechanics*, Innsbruck, 14-17 April 1988*: 2101-2108. Rotterdam: Balkema.

Cundall, P.A. & Lemos, J.V. 1990. Numerical simulation of fault instabilities with a continuously-yield joint model. In C. Fairhurst (ed.), *Proc. 2nd Int. Symp. on Rockbursts and Seismicity in Mines, Minneapolis, 8-10 June 1990*: 147-152. Rotterdam: Balkema.

Dietrich, J.H. 1978. Time-dependent friction and the mechanics of stick-slip. *Pure and Applied Geophysics* Vol. 116: 790-806.

Döring, T., Heinrich, F., Pforr, H. 1964. Zur Frage des Verformungs- und Festigkeitsverhaltens statistisch isotroper und homogener Gesteine mit inelastischen Verformungseigenschaften. In G. Bilkenroth & K.H. Höfer (eds), *Proc. 6th Int. Meeting of the Int. Bureau of Rock Mechanics, Leipzig, 3-7 November 1964*: 68-80. Berlin: Akademie.

IfG 2005. *Prognose der dynamischen Langzeitstabilität von Grubengebäuden im Salinar unter Berücksichtigung von Diskontinuitäts- und Schichtflächen*. Final report for Forschungszentrum Karlsruhe, FKZ 02C0892. Leipzig: Institut für Gebirgsmechanik.

Indraratna, B. & Haque, A. 2000. *Shear Behaviour of Rock Joints*. Rotterdam: Balkema.

Itasca 2005. *FLAC - Fast Lagrangian Analysis of Continua, Vers. 5.0*. Minneapolis: Itasca Consulting Group Inc.

Lux, K.H. 1984. *Gebirgsmechanischer Entwurf und Felderfahrungen im Salzkavernenbau.* Stuttgart: Enke.

Minkley, W. 1989. Festigkeitsverhalten von Sedimentgesteinen im post-failure-Bereich und Gebirgsschlagerscheinungen. In V. Maury & D. Fourmaintraux (eds), *Proc. Int. Symp. Rock at Great Depth, Pau, 28-31 August 1989, Vol. 1*: 59-65. Rotterdam: Balkema.

Minkley, W. 1997. Sprödbruchverhalten von Carnallitit und seine Auswirkungen auf die Langzeitsicherheit von Untertagedeponien. *Scientific reports 5*: 249-275. Karlsruhe: Forschungszentrum Karlsruhe.

Minkley, W., Mühlbauer, J., Storch, G. 2007. Dynamic processes in salt rocks - a general approach for softening processes within the rock matrix and along bedding planes. *In Proc. 6th Conference on the Mechanical Behaviour of Salt, Hannover, 22-25 May 2007*, in press. Rotterdam: Balkema.

Rice, J.R. 1983. Constitutive relations for fault slip and earthquake instabilities. *Pure and Applied Geophysics* Vol. 121: 443-475.

Ruina, A. 1983. Slip instability and state variable friction laws. *J. Geophys. Res.* 88: 10359-10370.

Salzer, K., Minkley, W., Popp, T. 2004. Safety assessment for the land surface in the vicinity of the potash shaft Neustassfurt VI. In H. Konietzky (ed.), *Proc. 1st Int. UDEC/ 3DEC Symposium, Bochum, 09/29-10/01 2004*: 113-119. Rotterdam: Balkema.

Spies, T., Hesser, J., Eisenblätter, J., Eilers, G. 2004. Monitoring of the rock mass in the final repository Morsleben: experiences with acoustic emission measurements and conclusions. In S. Jakusz (ed.), *Proc. Int. Conf. on Radioactive Waste Disposal, Berlin*, *26-28 April,* publ. on CD-ROM: 303-311. Hamburg: Kontec.

Swanson, P.L. & Boler, F.M. 1995. *The magnitude 5.3 seismic event and collapse of the Solvay Trona Mine: Analysis of pillar/floor failure stability.* U.S. Bureau of Mines, Open File Rept.: 86-95.